

DEVELOPMENT OF CRYOGENIC SUSPENSION IN THE ANU 8T SUPER-CONDUCTING SOLENOID WITH IRON YOKE

S. T. Battisson[†], T. B. Tunningley, N. R. Lobanov and D. Tsifakis, Department of Nuclear Physics, RSPE, Australian National University, Canberra, Australia
J. F. Smith, Department of Physics, University of Surrey, Guildford, UK

Abstract

An 8 Tesla superconducting solenoid was commissioned at The Australian National University to make precision measurements of fusion cross-sections. Forces between the solenoid and the iron yoke that houses it must always be maintained within safe limits and precision location of the solenoid coil is necessary to achieve this. Thermal contraction of components can impact the locating structure of the solenoid coil, leading to unsafe forces. Improvements to this structure allowed successful completion of the first fusion measurements with the 8T solenoidal separator, and demonstrated that it is now ready for a program of fusion measurements.

INTRODUCTION

A light radioactive ion beam (RIB) capability is being developed at the Australian National University (ANU). The basic design features of the separators, based on the superconducting solenoid with iron yoke, have recently been covered in Ref. [1-3]. The aim of the beam transport system is to efficiently transport and focus the secondary beam of interest onto the reaction target and suppress the undesired reaction products and intense scattered primary-beam projectiles. The ratio of undesired particles to particles of interest is 10^9 to 1. The high axial magnetic field (8T) produced by the superconducting solenoid coil will transport the elastically scattered beam particles back to the beam axis, either inside or beyond the solenoid. Evaporation residues, due to their larger magnetic rigidity, will be focused at a different (further) point. The 8.0 T superconducting magnet, manufactured by Oxford Instruments Omicron NanoScience, operates in dry, Cryofree® mode by conduction cooling using a cryo-cooler rather than bath cooling in liquid helium [4].

For applications in a separator, the magnetic field, at a certain distance away from the magnet aperture in the target and detector regions, should become sufficiently small since it is undesirable that (a) the direction of the beam and elastically scattered particles be affected and (b) the detector operation be influenced by the presence of the very strong magnetic field. Preventing a high magnetic field in regions external to the solenoid also minimises health and safety issues [5].

For small scale systems, the iron yoke over the coil has been found to be the most cost effective method of providing the required magnetic shielding. Moreover, the iron gets magnetized such that it adds to the central field generated by the coil. The magnet's cryostat shielded by an iron yoke is shown in Fig. 1.

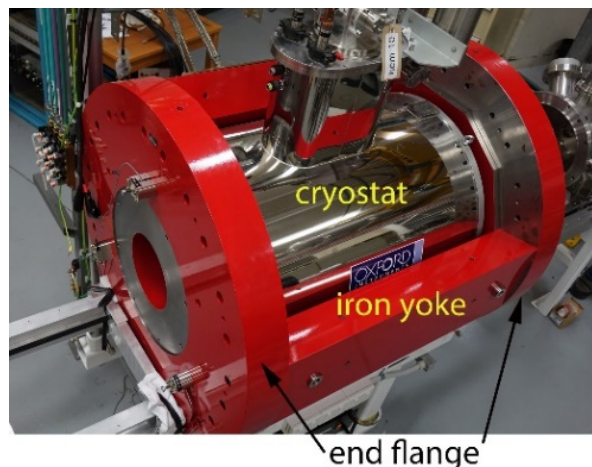


Figure 1: External view of device with upper bars of iron yoke and conical nose removed.

The yoke is made of 1010 steel which is a low carbon (0.08–0.13%) type. The 3.4 ton yoke includes two end flanges of 125 mm thickness and 925 mm diameter. The end flanges distribute the magnetic flux into eleven flux return bars which surround the magnet. In addition to the yoke, a 1010 steel plug is placed in the entrance to the solenoid reaching forward toward the target with the aim to minimise the change in trajectory of the elastically scattered beam particles travelling to the monitor detectors. The four monitor detectors are located in separate small chambers machined in the iron, pointing at the target. As a result of this cone, the magnetic field in the cylindrical apertures is ~ 15 G maximum while the field in the surrounding iron is about 10^4 G.

Such a cone cannot be used at the other end of solenoid, since, in some cases, the desired fusion products exit the solenoid with their focus at infinity i.e. parallel to the axis of the solenoid. The asymmetrical distribution of iron at the entrance and exit of the solenoid means that the coil would experience a net axial force if it was in the geometric centre of the yoke (radial forces are self-centring). To compensate for this force, the cryostat is offset along the axis of the iron yoke to balance the axial force when the cone for the original use of the solenoid is in place.

Mechanically the superconducting solenoid consists of four main components: cryostat, coils, supporting rods and iron shield. The coil, supported by radial and longitudinal rods, is mounted in a vacuum enclosure and shielded by a 50 °K cryogenically cooled super-insulated radiation shield. The axial and radial position of the cryostat inside the iron yoke can be adjusted by external means. The axial movement allows the elimination of out-of-balance forces

Any distribution of this work must maintain attribution to the author(s), title of the work, publisher, and DOI
 Content from this work may be used under the terms of the CC BY 3.0 licence © (© 2019).

on the solenoid. Cryogenic suspension requires specially dedicated design and set up especially when operating with the yoke.

The focus of this paper is an experimental verification of the cryogenic suspension of the superconducting coil in the magnet with iron yoke, aiming to achieve the required force balance generated by the magnetic field. This paper has been organised into three main sections. The first section outlines the cryogenic system and experimental procedure for reproducible measurement and logging of the magnetic forces over the entire temperature range. The second section presents key simulation and experimental results based on selected cooldowns and energising tests up to the required magnetic field of 8T. The third section presents interpretation of theoretical and experimental results and relating it to the performance of the separator under investigation.

METHODS

The superconducting coil is cooled to ~2.9K by means of a Sumitomo cryogenic cooler. Before cool-down is commenced, a vacuum of 5×10^{-4} Torr should be attained to provide insulation and remove condensable contaminants from the chamber. The cool-down process takes approximately 48 hours.

The code POISSON/SUPERFISH [6] was used to design and optimize the flux return iron geometry, ensuring minimum iron saturation at the maximum field setting of 8.0 T. The calculations that could be performed were sufficient to arrive at the design of the yoke and find out the balance point. The magneto-static problem consisted of seven different regions: air, five superconducting coils and the iron yoke. A variable permeability of iron region was linked to an internal table for 1010 steel [6]. A condition at the edges of the problem geometry were set to Dirichlet boundary when the field lines tend to be parallel to the boundary. The main goal of the simulation is the prediction of the magnet centre within the shield and accurate estimation of the magnetic force balance. This is dependent on the mechanical and magnetic symmetry of the shield along with the approximations made to enable a finite element analysis.

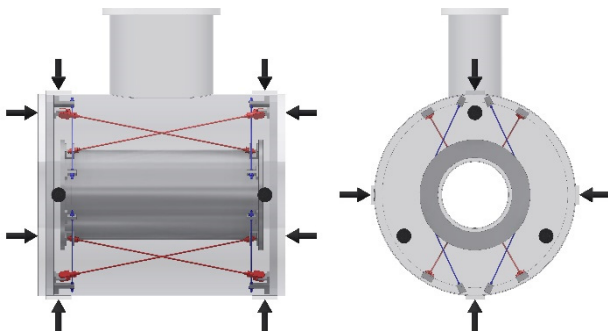


Figure 2: The coil, supported within the vacuum vessel by axial rods (red), radial rods (blue). Load cell constraint positions are shown in black.

The coil is firmly suspended and thermally isolated within the outer vacuum chamber of the cryostat by a series of 16 supporting rods made from G10 glass fibre. There

are 8 in the longitudinal direction and 8 in the radial. A simplified representation is shown in Fig. 2. The cryostat is constrained within the iron shield at 14 points – 6 in the axial direction and 8 radially. Load cells (Transducer Techniques LBC type) are used to monitor the forces acting between the solenoid coil and the iron shield. These load cells allow for accurate location and force measurement in all directions. The cells are ‘preloaded’ so that the solenoid is clamped tightly between them, and also so that they should never reach zero output.

Data logging and monitoring of the 8T system can be broken down into three main categories. They are i) magnet parameters (field as a function of power, and temperatures), ii) force measurement, and iii) beamline related parameters (valve positions, vacuum pressure, pump status). Over 40 separate process and calculated variables can be viewed in real-time via the ANU developed GUIs, Fig. 3, and are also recorded using the SLAC, BNL and FRIB developed EPICS Archiver Appliance. Experimental data is monitored and logged through a different system.



Figure 3: Solenoid control GUI, developed using EPICS EDM.

The magnet parameters are read directly to the EPICS system from an Ethernet connection to the Oxford Instrument NanoScience Mercury iPS power supply. Forces are measured by the 14 aforementioned load cells located at various positions in between the iron yoke and magnet vessel. These produce a 2mV/V output based on a 10V reference and are connected to an ANU-designed control box which houses a TS-7520 embedded computer, an ADAM 6017 ADC, a 5 port switch, and a 12V power supply and connects to the EPICS system via Ethernet. Vacuum is measured by a combination of Cold Cathode, Pirani, and Convectron gauging and sent through a serial to Ethernet converter to the EPICS system. Valve positions are read via ANU developed valve controllers.

RESULTS

Cool-down of the solenoid has been reliable and no issues have been encountered with the cryocooler or insulation of the coil. The coil reaches a temperature of 2.9K, which increases during energisation of the coil to a maximum of 3.9K but falls back to 3.0K when the current setting is static. Temperatures above 4K can cause the coil to quench, so efficient operation of the cooling system is critical.

B field profile on the solenoid axis z as a function of radius r and axial magnetic field distribution B_z are shown in Fig. 4.

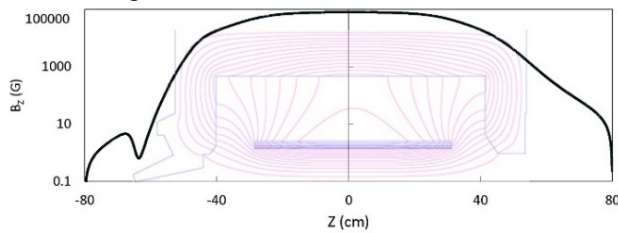


Figure 4: Magnetic field map on the z (horizontal) as a function of r (vertical logarithmic scale) plane and the magnetic field profile B_z on the solenoid axis.

The magnet coil-to-iron yoke positional relationship is very profound. Calculations of the force gradient indicates an approximately linear value of axial force $\Delta F_z/\Delta Z \approx 3\text{kN/mm}$ where ΔZ is the deviation from zero net force balance point. The typical calculated net axial force balance is shown in Fig. 5.

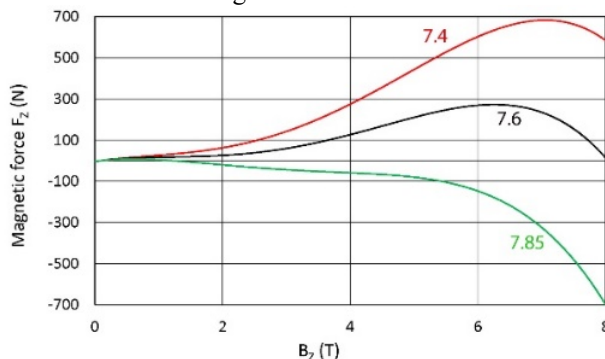


Figure 5: Calculated axial magnetic force balance F_z in 8T solenoid as a function of central flux density B_z . The graph trace labels represent solenoid offset ΔZ_{off} in mm from geometrical centre of yoke toward the conical nose.

The magnetic force depends on the magnetic field and the balanced net zero force position is achieved by displacement of the coil from the geometrical centre of the yoke toward the conical nose. The displacement (mm) is shown as a number next to the graph trace in Fig. 5.

During initial operation, no neutral point could be found where forces were balanced between the coil and the iron. Adjusting the position of the cryostat within the iron yoke by 0.01mm produced axial forces increasing beyond allowable limits in either direction. After increasing the tension of the axial tie rods by 2 mm, the balance point between coil and iron yoke could be established.

DISCUSSION AND CONCLUSION

Establishing the balance point required precise measurement of all forces. The control system allowed the monitoring of all important parameters in a convenient graphical user interface, Fig. 3.

The axial force under normal circumstances will go negative upon first ramping and, as the iron housing magnetically saturates, will turn and begin increasing, as shown in Fig. 5.

Due to the large forces possible from interaction between the coil and the iron yoke, the coil must be accurately positioned. Thermal contraction of the coil and suspension system components must be considered. In order to maintain coil position, the suspension system must always be exerting a larger restoring force than the attraction of the coil to the iron yoke. Tension in the suspension tie rods must be sufficient even when the coil has contracted in its cold state.

Experimental results indicated that tension was being lost in the axial rods when cold and the coil was moving out of position making the balance point impossible to locate. Tensioning of the rods allowed a proper restoring force to be exerted even when cold, stabilising the coil. With the coil accurately located within the iron, positional adjustment within 0.01mm was able to be conducted and the ideal position located.

ACKNOWLEDGEMENTS

This work has been supported by the Australian Federal Government Superscience/EIF funding under the NCRIS mechanism. We wish to express our appreciation to former technical staff Alistair Muirhead for his contribution at initial stage of this project.

REFERENCES

- [1] R. Rafiei, D.J. Hinde, M. Dasgupta, D.C. Weisser, A.G. Muirhead, A.B. Harding, A.K. Cooper, H.J. Wallace, N.R. Lobanov, A. Wakhle, M.L. Brown, C.J. Lin, A.J. Horsley, R. du Rietz, D.H. Luong, M. Evers, in *Nuclear Instruments and Methods*, vol. A631, p. 12, 2011.
- [2] A. Horsley, D. Hinde, M. Dasgupta, R. Rafiei, A. Wakhle, M. Evers, D. Luong, R. DuRietz., "Optimising conditions for production of ^6He , ^8Li , ^{10}Be and ^{12}B radioactive ion beams with the SOLEROO separator", in *Nuclear Instruments and Methods Section A*, vol. 646, no. 1, pp. 174-183, 2011.
- [3] M. Rodriguez, M. Brown, M. Dasgupta, D. Hind, D. Weisser, T. Kibedi, M. Lane, P. Cherry, A. Muirhead, R. Turkentine, N. Lobanov, A. Cooper, A. Harding, M. Blacksell, P. Davidson, "SOLITAIRE: A new generation solenoidal fusion product separator", in *Nuclear Instruments and Methods in Physics Research Section A* vol. 614, no. 1 pp. 119-129, 2010.
- [4] F.D. Becchetti, *et al.*, *Nuclear Instruments and Methods A* vol. 505, pp. 377, 2003.
- [5] John F. Schenck, "Safety of Strong, Static Magnetic Fields", *Journal of Magnetic Resonance Imaging*, vol. 12, pp. 2-19, 2000.
- [6] K. Halbach, R.F. Holisinger, *Particle Accelerators*, vol. 7, pp. 213, 1976.